Inorganic Chemistry

Article

pubs.acs.org/IC

Tris(2-pyridylborate) (Tpyb) Metal Complexes: Synthesis, Characterization, and Formation of Extrinsically Porous Materials with Large Cylindrical Channels

Chengzhong Cui, Patrick R. Shipman, Roger A. Lalancette,* and Frieder Jäkle*

Department of Chemistry, Rutgers University—Newark, 73 Warren Street, Newark, New Jersey 07102, United States

Supporting Information

ABSTRACT: Sandwich-like metal complexes $(Tpyb)_2M$ (M = Mg, Fe, Mn) that are based on the novel *t*-butylphenyltris(2-pyridyl)borate ligand were prepared and fully characterized by multinuclear NMR spectroscopy, high-resolution matrix-assisted laser desorption/ionization (MALDI) mass spectrometry, and single crystal X-ray crystallography. The unique steric and electronic nature of the Tpyb ligand led to structural parameters and properties that are quite different to those of previously reported tris(pyrazolyl)borate and tris(2-pyridyl)aluminate complexes. Most importantly, depending on the crystallization procedure, supramolecular structures could be generated with relatively smaller (ca. 4−5 Å) or larger (ca. 8 Å) diameter pores propagating throughout the crystal lattice. Although the supramolecular structures are held together only by weak intermolecular C−H···π interactions, the solvent in the larger channels could be completely removed without any loss of crystallinity or degradation of the framework. Surface area and gas uptake measurements on the Mg complex further confirmed the permanent porosity, while the calculated non-localized density functional theory (NLDFT) pore diameter of 8.6 Å proved to be in excellent agreement with that obtained from single crystal X-ray crystallography. Our new materials are remarkably thermally stable as degradation did not occur up to about 400 °C based on thermogravimetric analysis (TGA), and a sample of the Mg complex showed no loss of crystallinity even after heating to 140 °C under high vacuum for 72 h according to single crystal X-ray diffraction data.

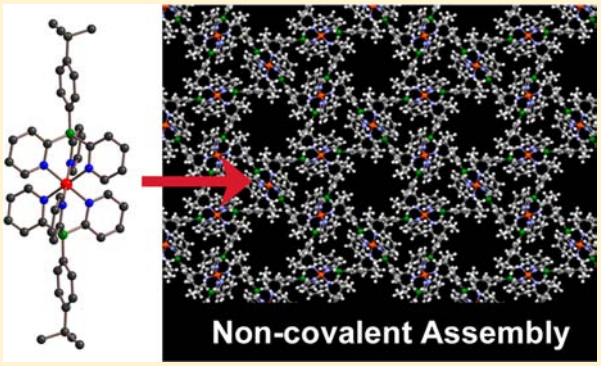

INTRODUCTION

Tris(1-pyrazolyl)borates (Tp, Chart 1) have evolved into one of the most useful classes of ligands in modern coordination chemistry.[1] Commonly referred to as "scorpionates" to reflect their distinct coordination geometry, they are potent ligands that complex essentially every metal in the periodic table. As uninegative tridentate six-electron donors, tris(1-pyrazolyl)-borates may also be viewed as analogues of cyclopentadienyls. One of the major advantages of pyrazolylborate ligands is their versatility derived from the different steric and electronic effects that are readily attained by varying the nature, number, and position of the substituents in the pyrazole rings. These second generation Tp ligands,[2] in which substituents on the pyrazolyl groups are introduced for steric and electronic fine-tuning, have been followed by a third generation ligand class, in which functional groups on the terminal (noncoordinated) substituent on boron provide for even greater diversity and tunability (Chart 1).[3,4] Consequently, these and related ligands have found widespread use in fields ranging from homogeneous catalysis to bioinorganic chemistry and materials science.[4,5]

We have recently introduced an alternative ligand design in which the pyrazolyl moieties in Tp are replaced with 2-pyridyl groups to form tris(2-pyridyl)borate (Tpyb) ligands.[6,7] An advantage of this new type of ligand is that the pyridyl groups are attached to boron through strong and only moderately polar B−C bonds. Moreover, the fact that pyridine is a better σ donor than pyrazole and that the steric requirements are different because of the use of six- rather than five-membered heterocycles has implications on potential applications not only in catalysis[8] but also in supramolecular chemistry, where tridentate ligands have had a remarkable impact.[9,10]

In this paper we describe in detail the complexation behavior of the tris(2-pyridyl)borate (Tpyb) ligand and the characterization of a range of octahedral metal complexes $(Tpyb)_2M$ (M = Mg, Fe, Mn). We also discuss the unexpected discovery of extended 3-dimensional structures with large channels. The creation of new porous materials that contain extended channels or cavities is among the most important targets in the field of crystal engineering because of their utility in the capture and storage of gases and other small molecules, separation science, catalysis and even fuel cells.[11] Typically these materials are stabilized by metal coordination, hydrogen bonding, or halogen-bonding interactions.[12] We introduce here a very rare example of "permanently porous"[13−16] molecular materials that, although held together solely based on C−H···π

Received: April 29, 2013
Published: August 5, 2013

   dx.doi.org/10.1021/ic4010664 | Inorg. Chem. 2013, 52, 9440−9448

Chart 1

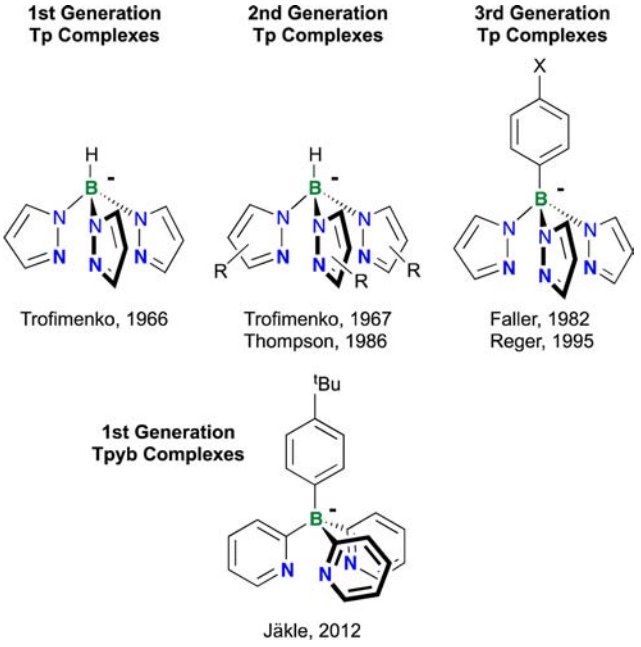

interactions, feature large cylindrical channels (diameters of ca. 8 Å) that proved to be stable even at temperatures in excess of 100 °C.

RESULTS AND DISCUSSION

The Tpyb ligand **1** was prepared by reaction of *t*-butylphenyl dibromoborane with 2-PyMgCl in CH_2Cl_2 at room temperature (RT) (Scheme 1). An aqueous Na_2CO_3 solution was

Scheme 1. Synthesis of Ligand 1 and Magnesium Complex 2-Mg

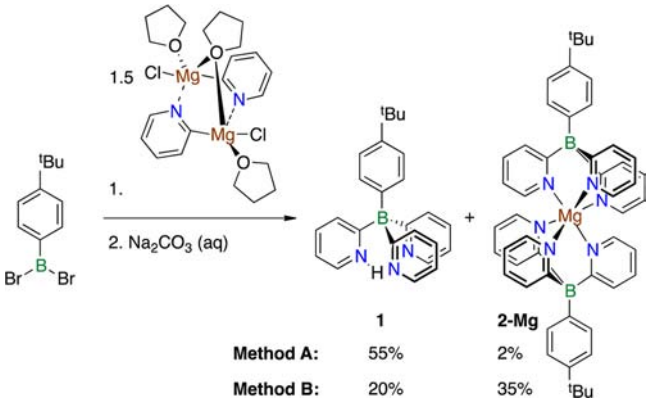

added, and the product extracted into CH_2Cl_2. The crude product was purified by column chromatography on NEt_3-deactivated silica gel using a mixture of acetone and hexanes as the eluent. Crystallization from toluene gave the analytically pure ligand **1** in its protonated form as a colorless solid in 54% yield.

During the synthesis of **1**, we noticed that a small amount of insoluble material remained after acetone extraction. This fraction showed a sharp peak in the ^{11}B NMR spectrum at a slightly different chemical shift (−9.2 vs −10.8 ppm for **1**). Extraction of the residue with dichloromethane and recrystallization from toluene afforded colorless crystals, which were identified by single crystal X-ray diffraction (vide infra) as the complex **2-Mg**. This complex can be obtained in higher yields of about 35% when the reaction is performed in toluene, the crude mixture evaporated to dryness, washed with hot MeOH and then cyclohexane. Alternatively, metal complexes of **1** can be generated by treatment of the free ligand with an appropriate metal salt in the presence of a base (Scheme 2).

Scheme 2. Synthesis of Metal Complexes 2-Fe and 2-Mn[a]

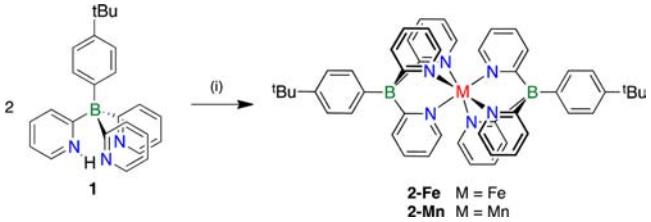

[a](i) MCl_2, NEt_3.

Treatment of **1** with $FeCl_2$ in THF/MeOH mixture containing about 3% NEt_3 gave **2-Fe** as a red solid that was purified by column chromatography and recrystallized from toluene. Similarly, reaction of **1** with $MnCl_2$ resulted in **2-Mn**, which was isolated as a light yellow solid. A small amount of hydrazine was added to the reaction mixture to prevent air oxidation of the metal ion.

While the ^{11}B NMR shifts of **1**, **2-Mg**, and **2-Fe** are very similar (Figure 1), the pattern of the pyridyl rings in the ^1H

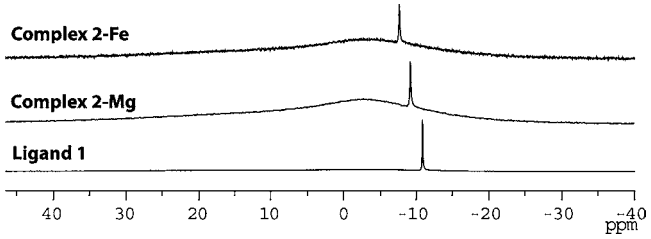

Figure 1. Overlay of ^{11}B NMR spectra of ligand **1**, complexes **2-Mg** and **2-Fe** in $CDCl_3$ (the broad features in **2-Mg** and **2-Fe** are due to borosilicate glass).

NMR changed dramatically as a result of the mutual shielding effect of the 6 pyridyl rings attached to the central Mg^{2+} ion. An overlay of the ^1H NMR spectra of the free ligand **1** and the Mg(II) and Fe(II) complexes is shown in Figure 2. The pyridyl protons in the ortho- and meta-positions to the ligating N experience characteristic upfield shifts from 8.49 to 7.58/7.11 (ortho) and 7.10 to 6.64/6.44 ppm (meta) upon going from the free ligand to the Mg/Fe complexes. Simultaneously, the phenylene protons are strongly shifted downfield. The assignments were confirmed by 2D NOESY NMR spectroscopy. The ^{13}C NMR spectra exhibit characteristic quartets at 150.3 ($J(^{11}B,^{13}C)$ = 55 Hz)/149.2 ($J(^{11}B,^{13}C)$ = 57 Hz) and 185.0 ($J(^{11}B,^{13}C)$ = 50 Hz)/188.0 ($J(^{11}B,^{13}C)$ = 50 Hz) ppm, which are due to coupling of the ^{11}B nucleus to the *ipso*-phenyl and *ipso*-pyridyl carbons, respectively. Complex **2-Mn** is paramagnetic, thus experiencing large shifts in both the ^{11}B (−109.6 ppm) and the ^1H NMR spectra (Supporting Information). The identity of each of the complexes was further confirmed by matrix-assisted laser desorption/ionization-time of flight (MALDI-TOF) mass spectrometry.

dx.doi.org/10.1021/ic4010664 | Inorg. Chem. 2013, 52, 9440−9448

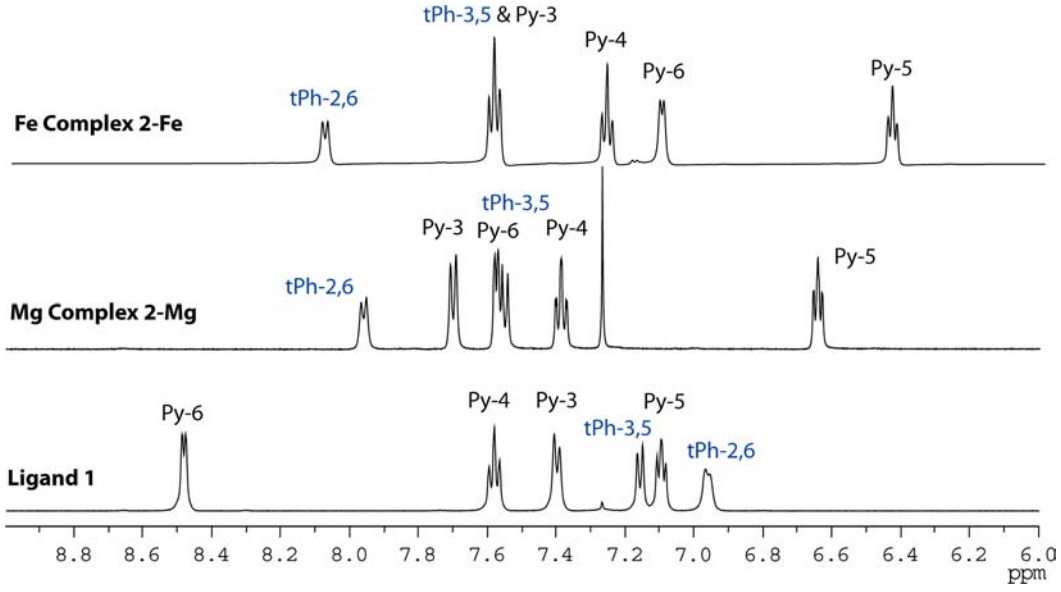

Figure 2. Comparison of ^{1}H NMR spectra (aromatic region) of ligand **1**, complexes **2-Mg**, and **2-Fe** in $CDCl_3$.

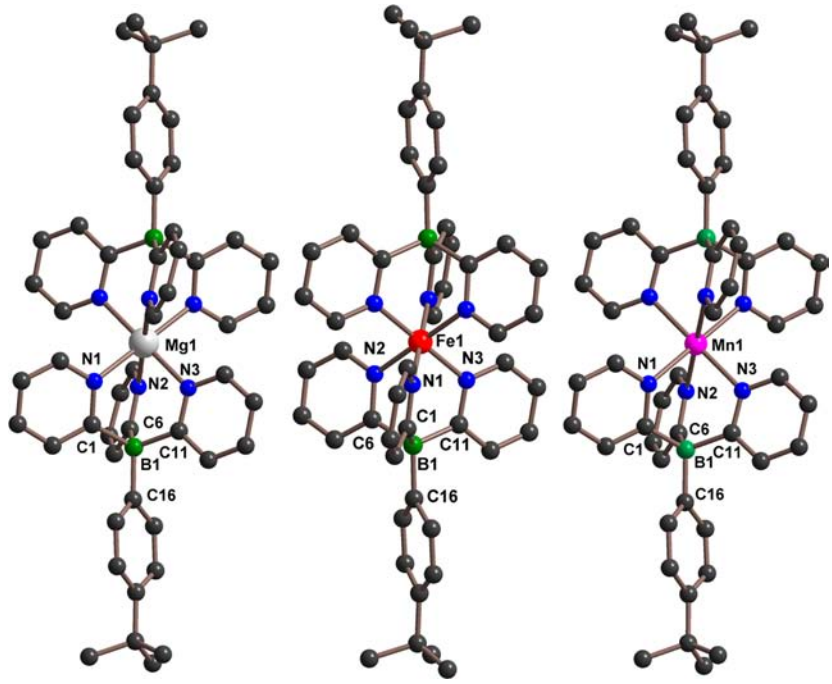

Figure 3. Ball-and-stick representations of the X-ray structures of **2-Mg**, **2-Fe**, and **2-Mn** (hydrogen atoms are omitted).

To study the coordination environment about the metal ion we performed single crystal X-ray diffraction analyses on crystals obtained by slow evaporation of toluene solutions (Figure 3). For **2-Fe** additional crystal samples were grown by slow solvent evaporation from CH_2Cl_2 and cyclohexane, respectively. The geometric features of the main molecules are quite similar to those of the toluene-grown crystals and hence not further discussed here. For all complexes the metal center lies on a crystallographic inversion center and adopts a slightly distorted octahedral geometry. Two of the M-N bonds are of similar length in each case (**2-Mg**: 2.1932(12) and 2.1916(11) Å, **2-Fe**: 1.9902(13) and 1.9880(13) Å, **2-Mn**: 2.268(2) and 2.265(2) Å), whereas the third one (**2-Mg**: 2.1322(16), **2-Fe**: 1.9685(13), **2-Mn**: 2.179(2) Å) is significantly shorter (see Table S1, Supporting Information). This distortion is also reflected in the ligand architecture. While for the free ligand **1** the C−B−C angles fall into a narrow range from 106.2−113.5°,[6] upon complexation a smaller angle is consistently observed between the more tightly bound pyridyl groups (C1−B1−C6 from 100.5(1)−101.8(1)°); the angles C1−B1−C11 and C1−B1−C16 (112.7(2)−116.0(2)°) to the phenyl group are correspondingly wider than the expected 109° in a perfect tetrahedral environment. These distortions appear to be related to steric interactions of the pyridyl hydrogens in *ortho*-position to the boryl group (H2, H7) with the *ortho*-hydrogens on the phenyl ring (H17, H21). The latter is adopting a position orthogonal to the more weakly bound pyridyl ring (N3 ring) but is positioned at relative small angles

dx.doi.org/10.1021/ic4010664 | *Inorg. Chem.* 2013, 52, 9440−9448

to the N1 and N2 rings. The N−Fe−N angles are close to 90° with a maximum deviation of 0.7°, whereas the variation of the N−Mg−N (86.0 to 94.0°) and N−Mn−N (84.0 to 96.0°) angles is somewhat larger, indicative of further geometric distortions. The pyridine nitrogens of one ligand are arranged coparallel to those of the second ligand with distances of 2.66 Å (**2-Mg**), 2.29 Å (**2-Fe**), and 2.80 Å (**2-Mn**), respectively, which increase with elongation of the M-N bonds. The phenyl rings are also positioned in a coparallel arrangement at fairly similar distances of 1.06 (**2-Mg**), 0.96 (**2-Fe**), and 1.08 Å (**2-Mn**) from one another.

A comparison of the M-N bond lengths to related complexes is insightful. For **2-Mn** the Mn−N bond distances of 2.179(2)−2.268(2) Å are somewhat shorter than those reported by Wright for the homologous aluminate complex $[Mn\{MeAl(2\text{-}py)_3\}_2]$[17] (2.291(3)−2.305(3) Å). Nonetheless, they are well within in the range of Mn−N bond distances reported in the literature for Mn(II) d^5 high-spin complexes with tridentate N ligands.[18] A high spin configuration is also consistent with the light yellow color of the compound and the large chemical shifts in the ^{1}H NMR spectra. As in the case of the Mn species, the Fe−N bonds of 1.9685(13)−1.9902(13) Å for **2-Fe** are shorter than those for the corresponding charge-neutral high-spin complex $[Fe\{MeAl(2\text{-}py)_3\}_2]$ (Fe−N average of 2.054(3) Å[17]). They are, however, comparable to or only slightly longer than the ones in diamagnetic tripodal iron complexes with N or C as the bridgehead atom ($[Fe\{N(2\text{-}py)_3\}_2]^{2+}$: Fe−N = 1.970(5)−1.995(5) Å[19]; $[Fe\{HC(2\text{-}py)_3\}_2]^{2+}$: Fe−N = 1.947(2)−1.954(2) Å[20]). Also on the basis of the NMR evidence, we conclude that both in solution and in the solid state **2-Fe** adopts a low spin configuration. Our results further indicate that the size of the bridgehead atom (Al vs B) has a critical influence on the electronic structure of these Fe(II) complexes.

Supramolecular Structures. Based on the discussions above the structural features of complexes **2-M** (M = Mg, Fe, Mn) are quite similar; however, **2-Fe** crystallized from toluene in the monoclinic space group $C2/c$ whereas **2-Mg** and **2-Mn** crystallized in the more highly symmetric hexagonal space group $R\bar{3}$. When further examining the crystal packing, we were surprised to discover that all these complexes adopt supramolecular structures with channels that run through the crystal lattice along the crystallographic *b*- (**2-Fe**) or *c*-axis (**2-Mg** and **2-Mn**). In the case of the toluene solvate **2-Fe**(C_7H_8), a layered structure is evident in which the metal complexes alternate with layers made up of the *t*-butylphenyl groups and the cocrystallized toluene molecules (Figure 4). The solvent channels are oriented perpendicular to these layers; they are rhomboid-shaped and have relatively small diameters (the shortest H···H distances across the channels are about 5.5 and 4.4 Å). There are 4 channels per unit cell, each of them accommodating one toluene molecule per main molecule.

In contrast, for **2-Mg** and **2-Mn** large hexagonal channels (3 channels per unit cell, 9 main molecules) with a diameter of about 8 Å were observed (Figure 5).[17,21,22] In an attempt to generate a porous structure of **2-Fe** similar to the one adopted by **2-Mg** and **2-Mn**, we examined a range of different solvents and conditions for crystallization. Indeed, when we crystallized **2-Fe** by slow solvent evaporation of a solution in CH_2Cl_2 or cyclohexane, we succeeded in obtaining single crystals in the $R\bar{3}$ space group that feature pores similar to those in **2-Mg** and **2-Mn**.

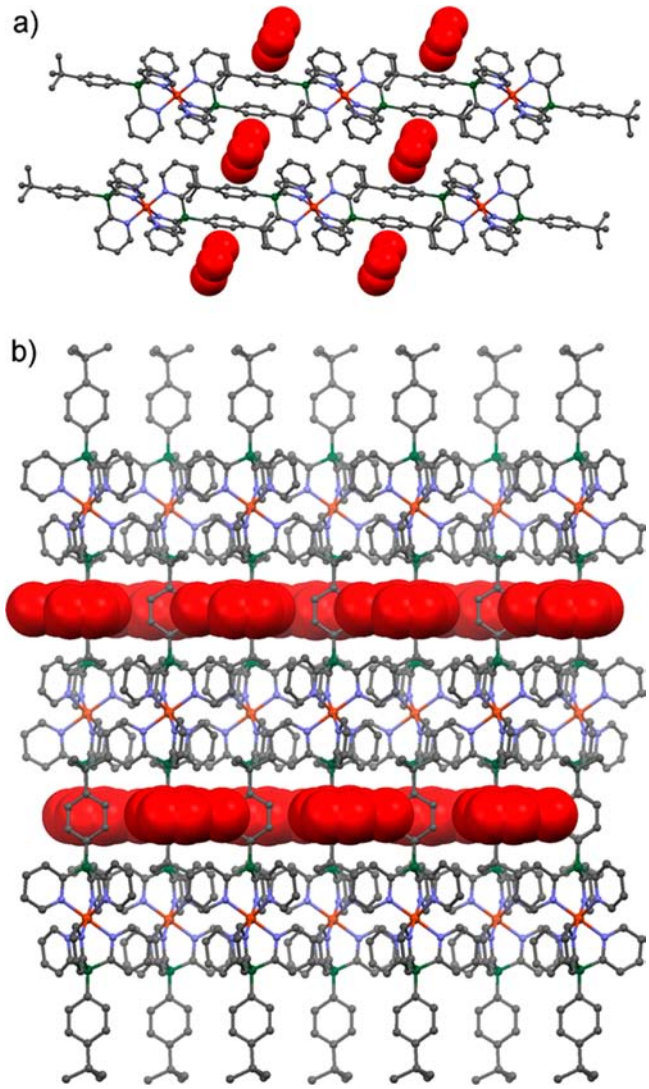

Figure 4. Perspective views of the extended structure of **2-Fe**(C_7H_8) along the crystallographic *b*-axis (top) and *a*-axis (bottom); B: green, N: blue, Fe: orange, toluene molecules: red; H atoms are omitted.

The different complexes are isostructural and the channel sizes vary only slightly with changes in the central metal ion or the nature of the cocrystallized solvent. The pore sizes were estimated by measuring the shortest H···H distances across the channels to be 8.99 Å for **2-Mg**$(C_7H_8)_x$; 8.98 Å for **2-Mn**$(C_7H_8)_x$; 8.88 Å for **2-Fe**$(C_6H_{12})_x$; and 8.89 Å for **2-Fe**$(CH_2Cl_2)_x$ (the effective diameters are somewhat smaller when taking the H van der Waals radii into consideration). The individual channels are generated by alternate packing of 3 metal complexes that are rotated by 60° from layer to layer. As illustrated in Figure 6, the third layer (light blue) is positioned in the next unit cell and coincides with the positioning in the first layer (dark blue). There is some overlap between the phenyl rings in one layer and the pyridyl rings of the next layer and vice versa. This leads to sandwich-like arrangements, in which two pyridyl rings (blue) show C−H···π contacts to a phenyl ring (green), whereas two phenyl rings (blue) of the adjacent molecules in the same layers show C−H···π contacts to a pyridyl ring (green) positioned in-between them. The Ph-to-Py C−H···π distances differ slightly from compound to compound, which is primarily due to slight differences in the

dx.doi.org/10.1021/ic4010664 | Inorg. Chem. 2013, 52, 9440−9448

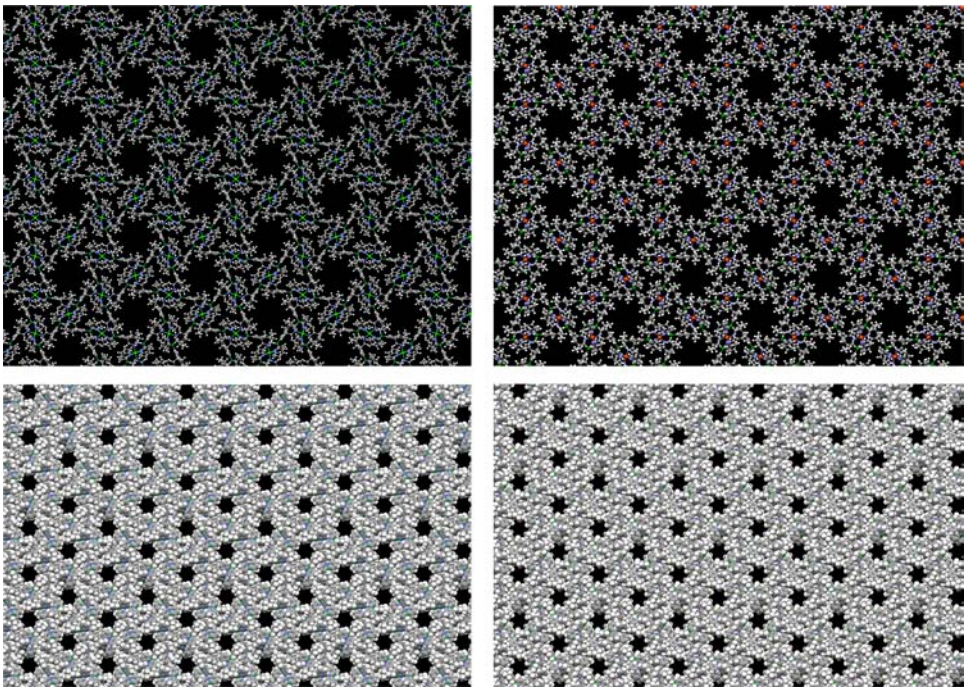

Figure 5. Ball-and-stick and space filling views of the extended structures of **2-Mg**$(C_7H_8)_x$ (left) and **2-Fe**$(C_6H_{12})_x$ (right) along the crystallographic *c*-axis; diffuse solvent molecules were removed using the SQUEEZE routine in Platon.[23]

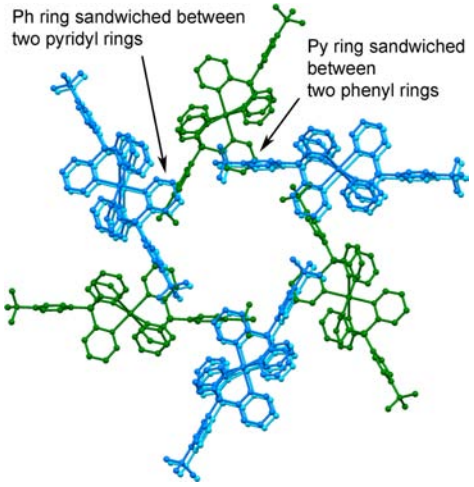

Figure 6. Illustration of the formation of hexagonal channels in **2-Mg**$(C_7H_8)_x$.

relative orientation of the aromatic groups (**2-Mg**$(C_7H_8)_x$ 3.155, 3.341; **2-Mn**$(C_7H_8)_x$ 3.121, 3.381; **2-Fe**$(C_6H_{12})_x$ 3.228, 3.348; **2-Fe**$(CH_2Cl_2)_x$ 2.877, 3.284 Å; the C−H distances were fixed at 0.95 Å in all cases). They are in the range of, or slightly longer that, typically observed for strong C−H···π interactions ($\leq$3.05 Å).[24]

In the case of the crystals grown from CH_2Cl_2, 18 solvent molecules per unit cell were found in well-defined positions in the channels. Their occupancy was refined to about 0.25; a positional disorder is expected given the relative orientation and very close contact between the CH_2Cl_2 molecules (see Figure S6, Supporting Information, and Table 1). Considering the crystal symmetry, it is possible that partial solvent loss occurred, and the actual occupancy of a fully solvated crystal could well be larger, up to a theoretical maximum of one CH_2Cl_2 molecule per main molecule, which corresponds to full occupation of every other site. The incorporated solvent molecules in **2-Fe**$(C_6H_{12})_x$ proved to be diffuse and had to be treated using the "SQUEEZE" routine in the program Platon.[23] Similarly, the solvent molecules in **2-Mg**$(C_7H_8)_x$ and **2-Mn**$(C_7H_8)_x$ were not well localized. Importantly, the solvent-accessible volume based on the Platon SQUEEZE routine is similar in **2-Mg**$(C_7H_8)_x$ (1829 Å^3) and **2-Mn**$(C_7H_8)_x$ (1864 Å^3), and just slightly larger than in **2-Fe**$(C_6H_{12})_x$ (1643 Å^3).

We performed thermogravimetric analyses (10 °C/min) on all complexes to quantitate the amount of solvent that is present and to determine suitable conditions for solvent removal without decomposition. The TGA trace of **2-Fe**(toluene) showed a sharp 10.8% weight loss at an onset temperature of 130 °C (midpoint of 135 °C; see Figure 7). This result is consistent with loss of all cocrystallized toluene molecules, indicative of facile desorption from the crystal at the boiling point of toluene because of a lack of specific interactions. In contrast, the loss of toluene from the hexagonal channel-like structures of **2-Mg**(toluene)$_x$ and **2-Mn**(toluene)$_x$ occurred much more gradually, over a temperature range from about 100 to 250 °C. The weight loss for **2-Mg**(toluene)$_x$ and **2-Mn**(toluene)$_x$ corresponded to about 5 and 6 toluene molecules per unit cell (9 main molecules), respectively, which correlates well with an expected 2 toluene molecules in each of the 3 channels when the structure is fully solvated. Similarly, for **2-Fe**$(CH_2Cl_2)_x$, the TGA measurements showed a very gradual loss of about 1 molecule of CH_2Cl_2 per main molecule, which is significantly more than the amount determined by X-ray crystallography (x = 0.5). This apparent discrepancy is readily explained by partial desolvation of the crystal used for X-ray structure determination. The sample used for TGA was isolated immediately prior to the measurement, and the TGA trace indicates facile partial solvent loss close to room temperature.

Over the course of our studies we discovered that the single crystals that adopt channel-like structures retained their

dx.doi.org/10.1021/ic4010664 | *Inorg. Chem.* 2013, 52, 9440−9448

Table 1. Comparison of Crystal Data and Thermogravimetric Analysis (TGA) Results for Microporous Channel-Like Structures of 2-M (M = Mg, Fe, Mn)

	2-Fe(C_7H_8)	**2-Mg**$(C_7H_8)_x$	**2-Mn**$(C_7H_8)_x$	**2-Fe**$(CH_2Cl_2)_x$	**2-Fe**$(C_6H_{12})_x$
Z (main molecule)	4	9	9	9	9
MW (main molecule)	812.43	780.89	811.52	812.43	812.43
MW (solvent)	$(92.14)_1$	$(92.14)_x$	$(92.13)_x$	$(84.93)_x$[d]	$(84.16)_x$
ρ_{calc}, g cm^{-3}[a]	1.320	1.062	1.100	1.188[d]	1.133
V, Å^3	4553.1(1)	10984.6(6)	11021.9(2)	10759.9(7)	10717.6(7)
solvent-accessible V (Platon), Å^3	e	1829	1864	e	1643
TGA T_{onset} (°C, 1st step)[b]	130	ca. 100	ca. 100	ca. 50	e
TGA $T_{1/2}$ (°C, 1st step)[c]	135	190	210	195	e
TGA % weight loss (1st step)	10.8	6.3	7.6	10.2	e
TGA solvent molecules x per main molecule	0.95[f]	0.54	0.67	0.98	e
TGA T_{onset} (°C, 2nd step)[b]	430	395	410	425	e
TGA $T_{1/2}$ (°C, 2nd step)[c]	440	410	430	430	e

[a]The crystal density is calculated based on solvent-filled channels for **2-Fe**(C_7H_8) and **2-Fe**$(CH_2Cl_2)_{0.5}$ and for empty channels for all other structures. [b]Onset of solvent loss (1st step) or thermal degradation (2nd step). [c]50% weight loss temperature for the specified step. [d]For **2-Fe**$(CH_2Cl_2)_x$ the refined occupancy is about 0.25, corresponding to 0.25 × 18 solvents per 9 main molecules in the unit cell; i.e., x = 0.5. [e]Not determined. [f]Crystals were freshly prepared prior to measurement.

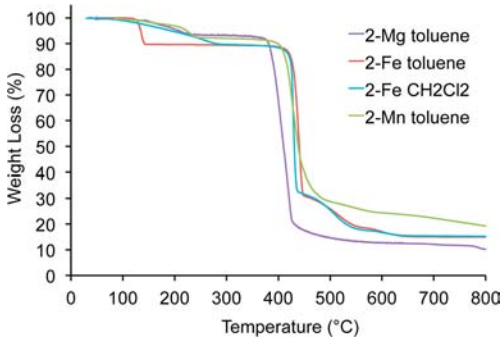

Figure 7. Comparison of TGA data for **2-Mg**$(C_7H_8)_x$, **2-Fe**(C_7H_8), **2-Mn**$(C_7H_8)_x$, and **2-Fe**$(CH_2Cl_2)_x$; all data acquired at a scan rate of 10 °C/min.

appearance even at elevated temperatures and after prolonged exposure to air (>1 year in some cases). This suggested that solvent loss occurred without degradation, a phenomenon commonly referred to as permanent porosity. Permanently porous materials are relatively common for metal−organic frameworks (MOFs) and covalent organic frameworks (COFs), but they remain exceedingly rare for porous materials based on molecular compounds. This is especially true when the molecular structure itself does not feature any void spaces: so-called extrinsic porous materials.[14,25] The main reason is that the lack of strong intermolecular interactions typically results in facile structural collapse upon evaporation of cocrystallized solvent molecules. The phenomenon of extrinsic permanently porous organic solids was first confirmed for tris-(phenylenedioxy)-cyclophosphazene (TPP).[26] A focused search by several research groups for other examples of such materials has resulted in the discovery of a range of new compounds over the past several years, including dipeptides, silylated biphenyl species, phthalocyanines, and triptycene derivatives.[16,27−31] The observation of relatively large pores in some of these materials has attracted considerable interest regarding not only gas sorption but also separation and even catalytic applications.[27,32]

To establish the permanent porosity of our compounds we acquired X-ray diffraction data of a freshly crystallized sample of **2-Mg**$(C_7H_8)_x$ before and after heating under high vacuum to 115 °C for 24 h and subsequently to 140 °C for 72 h. Comparison of the X-ray data demonstrated the integrity of the crystal and channel structure upon removal of solvent as illustrated by a very small change in the cell parameters with decreasing amount of trapped solvent (Supporting Information, Table S3). While the trapped solvent could not be refined, we were able to judge the loss of solvent based on the residual electron density during refinement. For example, for the freshly crystallized sample, the strongest residual peak upon refinement of the main molecule was due to the solvent (toluene) and had an intensity of 1.41, whereas the strongest H of the main molecule had an intensity of 0.51. After heating to 115 °C for 24 h both the residual solvent and the strongest hydrogen on the main molecule had the same intensity at 0.73 with no change in the cell parameters. The intensity of the solvent peak decreased further to 0.63 after evacuation at 140 °C for 72 h, indicating significant loss of trapped solvent with little change in the cell parameters. The remaining intensity might be due to uptake of gas or small molecules from the atmosphere during crystal mounting (the crystals were mounted without the use of oil in a glass capillary).

We further examined the porosity of **2-Mg** by means of gas sorption measurements (Figure 8). For this purpose, the solvent of a sample of **2-Mg**$(C_7H_8)_x$ was exchanged with *n*-pentane (3 × 24 h) and the material was then evacuated for 20

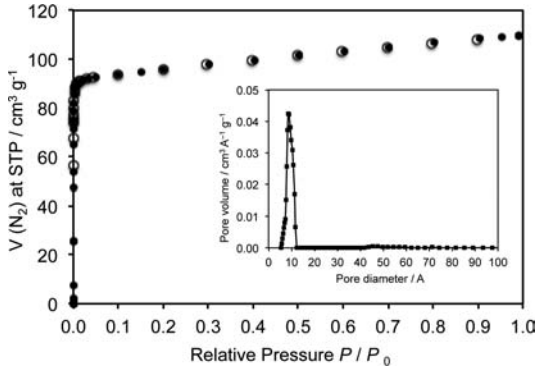

Figure 8. Nitrogen sorption isotherm of **2-Mg** at 77K. ● adsorption, ○ desorption. The inset shows the NL-DFT pore-size distribution.

dx.doi.org/10.1021/ic4010664 | Inorg. Chem. 2013, 52, 9440−9448

h while heating to 100 °C. Based on 77 K N_2 sorption measurements, the Brunauer–Emmett–Teller (BET) surface area was 290 m^2/g and the Langmuir surface area 431 $m^2\ g^{-1}$. A micropore volume V_{mp} = 0.168 mL g^{-1} was determined. The surface area and pore volume are in a similar range as for the relatively few other previously reported extrinsically porous molecular organic solids.[16,27,28] They are however lower than those of McKeown's phthalocyanine unsolvated nanoporous crystals (PUNCs)[29] and the record of about 2796 $m^2\ g^{-1}$ and V_{mp} = 1.02 mL g^{-1} for triptycenetrisbenzimidazolone (TTBI) very recently reported by Mastalerz.[31]

Pore size analysis using the non-localized density functional theory (NLDFT) model revealed a single narrow distribution of pores with a diameter of 8.6 Å, which is in excellent agreement with the crystal structure data. This is larger than for most reported molecular organic solids and even larger than the predominant pores reported for TTBI,[31] although the latter shows some additional pores that are >10 Å in diameter. Noteworthy is also that the structures in our workare clearly microporous with large channels, despite the fact that they do not satisfy the criterion of a calculated density of <0.9 g cm^{-3} put forward by McKeown and co-workers[33] in their search for new microporous organic solids. This can be understood when considering the incorporation of (heavier) metal atoms in the actual molecular structure and the relatively dense packing of the molecules around the hexagonal channels that does not give rise to additional smaller void spaces. We also performed preliminary studies on the sorption of other gases (Figure S7, Supporting Information). Adsorption of about 8 mL g^{-1} CO_2 (1.55 wt %) at 25 °C and about 4 mL g^{-1} of CH_4 (0.28 wt %) at 0 °C was observed, respectively.

CONCLUSIONS

Utilizing the novel pyridylborate ligand Tpyb we prepared and fully characterized a range of sandwich-like complexes with different central metal ions. We introduced two different synthetic pathways to these novel metal complexes. In comparison to previously reported pyrazolylborate and pyridylaluminate complexes significantly different structures and properties were observed. Interestingly, we discovered the formation of supramolecular 3-D structures with unusually large channels. Extrinsic porous molecular crystals have attracted much interest in recent years, but remain exceedingly rare, because the interactions that hold the framework together are typically weak and structural collapse tends to occur readily.[14−16] We succeeded in completely removing the solvent by direct thermal treatment under high vacuum or after exchange of the solvent with *n*-pentane. Compared to most other extrinsically porous molecular materials the channel sizes in our compounds are significantly larger. The surface area and gas uptake measurements on **2-Mg** further confirmed the permanent porosity, while the calculated NL-DFT channel size proved to be consistent with that from single crystal X-ray crystallography. The thermal stability of our new materials is remarkable: thermal degradation of compounds **2-M** did not occur up to about 400 °C based on TGA, and a sample of **2-Mg** showed no loss of crystallinity after heating to 140 °C under high vacuum for 72 h according to X-ray diffraction analysis data. This stands in sharp contrast to most previously reported molecular organic solids, which tend to either display low melting points and/or undergo phase changes at relatively low temperatures. Finally, a unique aspect of our materials in comparison to those based on purely organic materials is the presence of metal centers that provide for potentially interesting optical, redox, electronic, magnetic, and sensory properties. Further efforts at taking advantage of these properties are in progress, as are attempts at introducing metal complexes based on appropriately substituted "2nd and 3rd generation" pyridylborate ligands to create new functional materials.

EXPERIMENTAL SECTION

Materials and General Methods. Mg, 2-bromopyridine, and NEt_3 were purchased from Fisher Scientific, $MnCl_2$ and $FeCl_2$ (anhydrous) from Sigma-Aldrich. 4-*t*-Butylphenyl dibromoborane was prepared according to a literature procedure.[34] Solvents were purchased from Pharmco and used as received unless noted otherwise. Ether solvents were distilled from Na/benzophenone prior to use. Hydrocarbon and chlorinated solvents were purified using a solvent purification system (Innovative Technologies; alumina/copper columns for hydrocarbon solvents). Chlorinated solvents were distilled from CaH_2 and degassed via several freeze–pump–thaw cycles. Reactions and manipulations involving boron halide species were carried out under an atmosphere of prepurified nitrogen using either Schlenk techniques or an inert-atmosphere glovebox (Innovative Technologies). All other procedures were carried out under ambient conditions.

The 499.9 MHz ^{1}H NMR, 125.7 MHz ^{13}C NMR, and 160.4 MHz ^{11}B NMR spectra were recorded on a Varian INOVA 500 MHz spectrometer equipped with a boron-free probe. All ^{1}H NMR and ^{13}C NMR spectra were referenced internally to the solvent peaks and ^{11}B NMR spectra to $BF_3{\cdot}Et_2O$ (δ = 0) in C_6D_6. The assignments are based on the numbering scheme shown here.

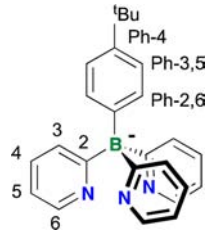

The MALDI-TOF measurements were performed on an Applied Biosystems 4800 Proteomics Analyzer in reflectron (+) or (−)-mode with delayed extraction. For data acquisition in (+)-mode benzo[α]-pyrene was used as the matrix (20 mg/mL in toluene) and in (−)-mode α-cyano-4-hydroxycinnamic acid (50% acetonitrile, 0.1% TFA in deionized water). The sample was dissolved in toluene or MeOH (ca. 10 mg/mL), mixed with the matrix in a 1:10 ratio, and then spotted on the wells of a sample plate. High resolution MALDI-MS data (benzo[α]pyrene matrix) were obtained on an Apex Ultra 7.0 Hybrid FTMS (Bruker Daltonics).

TGA data were acquired on a Perkin-Elmer Pyris 1 Thermogravimetric Analyzer at a scan rate of 10 °C/min. Elemental analyses were performed by Quantitative Technologies, Inc., Whitehouse, NJ. Surface area and gas sorption measurements were performed on a Quantachrome Autosorb-1C instrument.

Single crystal X-ray diffraction intensities were collected on a Smart Apex2 CCD diffractometer at 100 K using Cu Kα (1.54178 Å) radiation and details of the X-ray diffraction experiments and crystal structure refinements are given in Supporting Information, Tables S1 and S2. The crystals were mounted on a loop using Paratone-N oil with the exception of the structure analysis of **2-Mg** described in Supporting Information, Table S3 (sealed capillary). The structures were solved by direct methods and refined by full-matrix least-squares based on F^2 with all reflections.[35] Non-hydrogen atoms were refined with anisotropic displacement coefficients, and hydrogen atoms were treated as idealized contributions. SADABS[36] numerical face-indexed absorption was applied. Diffuse solvent contributions were treated using the program Platon.[23] Crystallographic data for the structures of **2-Fe**(C_7H_8), **2-Mg**$(C_7H_8)_x$, **2-Fe**$(CH_2Cl_2)_{0.5}$, **2-Fe**$(C_6H_{12})_x$, and **2-**

dx.doi.org/10.1021/ic4010664 | Inorg. Chem. 2013, 52, 9440−9448

Mn$(C_7H_8)_x$ have been deposited with the Cambridge Crystallographic Data Center as supplementary publications CCDC-878728, 931934–931937, respectively. Copies of the data can be obtained free of charge on application to CCDC, 12 Union Road, Cambridge CB2 1EZ, U.K. (fax: (+44) 1223-336-033; email: deposit@ccdc.cam.ac.uk).

Synthesis of *t*-Butylphenyltris(2-pyridyl)borate Free Acid (1). *t*-Butylphenyl dibromoborane (5.00 g, 16.5 mmol) in CH_2Cl_2 (30 mL) was added dropwise to a solution of pyridyl Grignard (14.5 g, 25.7 mmol) in CH_2Cl_2 (50 mL). The resulting dark red mixture was kept stirring for 5 h. The reaction mixture was poured into an aqueous Na_2CO_3 solution (30 g in 250 mL H_2O) to give a slurry which was stirred for 30 min. Extraction with CH_2Cl_2 (3 × 200 mL) gave a brown organic phase that was dried over Na_2SO_4. The solvents were removed under vacuum to give an oil that was redissolved in acetone (100 mL), filtered, and brought to dryness. The product was further purified by chromatography on silica gel with a 1:1 mixture of hexanes and acetone containing 1% (v/v) triethylamine as the eluent. The product was dried under high vacuum at 60 °C for 10 h to give a white solid. Yield: 3.4 g (54%). ^{1}H NMR (499.973 MHz, $CDCl_3$) δ = 19.5 (br s, 1H, pyridyl N–H), 8.49 (d, ^3J = 5.0 Hz, 3H, pyridyl-H6), 7.58 (pst, ^3J = 7.5 Hz, 3H, pyridyl-H4), 7.40 (d, ^3J = 7.5 Hz, 3H, pyridyl-H3), 7.16 (d, ^3J = 7.5 Hz, 2H, tPh-H3,5), 7.10 (pst, ^3J = 6.3 Hz, 3H, pyridyl-H5), 6.96 (br d, ^3J = 6.0 Hz, 2H, tPh-H2,6), 1.27 (s, 9H, *t*-Bu). ^{13}C NMR (125.718 MHz, $CDCl_3$) δ = 184.2 (q, $^1J_{C-B}$ = 53.1 Hz, pyridyl-C2), 152.3 (q, $^1J_{C-B}$ = 50.0 Hz, tPh–C1), 146.9 (tPh–C4), 143.6 (pyridyl-C6), 136.3 (pyridyl-C4), 134.2 (tPh–C2,6), 131.8 (pyridyl-C3), 124.2 (tPh–C3,5), 119.8 (pyridyl-C5), 34.3 ($C(CH_3)_3$), 31.7 ($C(CH_3)_3$). ^{11}B NMR (160.386 MHz, $CDCl_3$) δ = −10.8 ($w_{1/2}$ = 13 Hz). MALDI-TOF MS (benzo[α]pyrene): m/z = 380.233 (MH^+, calcd for $^{12}C_{25}{}^1H_{27}{}^{11}B_1{}^{14}N_3$ 380.313). Elemental analysis: calcd for $C_{25}H_{26}B_1N_3$: C 79.16, H 6.91, N 11.08%; found C 78.92, H 6.94, N 11.08%. Single crystals for X-ray diffraction analysis were obtained by slow evaporation of a toluene solution.

Synthesis of Bis(*t*-butylphenyltris(2-pyridyl)borate) Magnesium (2-Mg). A solution of *t*-butylphenyl dibromoborane (1.0 g, 3.3 mmol) in toluene (15 mL) was slowly added to a solution of pyridyl Grignard (2.9 g, 5.4 mmol) in toluene (40 mL). The reaction mixture was stirred for 12 h and then brought to dryness under high vacuum to give a white solid residue. Methanol (300 mL) was added, and the mixture was refluxed for 1 h. The product was collected by filtration, washed with cyclohexane, and then dried under high vacuum. Yield: 0.45 g (35%). ^{1}H NMR (499.973 MHz, $CDCl_3$) δ = 7.97 (d, ^3J = 7.5 Hz, 4H, tPh-H2,6), 7.70 (d, ^3J = 8.0 Hz, 6H, pyridyl-H3), 7.58 (d, ^3J = 5.5 Hz, 6H, pyridyl-H6), 7.56 (d, ^3J = 8.0 Hz, 4H, tPh-H3,5), 7.39 (pst, ^3J = 7.5 Hz, 6H, pyridyl-H4), 6.64 (pst, ^3J = 6.3 Hz, 6H, pyridyl-H5), 1.51 (s, 18H, *t*-Bu). ^{13}C NMR (125.718 MHz, $CDCl_3$) δ = 185.0 (q, $^1J_{C-B}$ = 50 Hz, pyridyl-C2), 150.3 (q, $^1J_{C-B}$ = 55 Hz, tPh–C1), 148.4 (pyridyl-C6), 147.2 (tPh–C4), 137.0 (tPh–C2,6), 134.9 (pyridyl-C4), 129.9 (pyridyl-C3), 124.3 (tPh–C3,5), 118.7 (pyridyl-C5), 34.6 ($C(CH_3)_3$), 32.0 ($C(CH_3)_3$). ^{11}B NMR (160.411 MHz, $CDCl_3$) δ = −9.2 ($w_{1/2}$ = 18 Hz). MALDI-TOF (benzo[α]pyrene): m/z = 780.415 (M^+, calcd for $^{12}C_{50}{}^1H_{50}{}^{11}B_2{}^{24}Mg_1{}^{14}N_6$ 780.413). Elemental analysis (dried under vacuum at 80 °C overnight): calcd for $C_{50}H_{50}B_2Mg_1N_6$: C 76.90, H 6.45, N 10.76%; found C 76.44, H 6.45, N 10.68%. Single crystals for X-ray diffraction analysis were obtained by slow evaporation of solutions prepared in dry toluene at 50 °C or in CH_2Cl_2 at room temperature, respectively.

The methanol filtrate from the above workup procedure was concentrated to about 10 mL and then CH_2Cl_2 (100 mL) was added. The resulting solution was poured into an aqueous Na_2CO_3 solution (20 g, 150 mL), the organic layer was isolated and the aqueous layer was extracted with CH_2Cl_2 (2 × 50 mL). The combined organic layers were dried over Na_2SO_4, concentrated and purified by column chromatography on silica gel with solvent gradients ranging from hexanes to acetone containing 1% (v/v) triethylamine. The product was isolated by evaporation of the solvents and identified by NMR spectroscopy to be the free acid **1**. Yield: 0.25 g (20%).

Synthesis of Bis(*t*-butylphenyltris(2-pyridyl)borate) Iron(II) (2-Fe). A 100 mL Schlenk flask was charged with anhydrous $FeCl_2$ powder (0.10 g, 0.79 mmol) and anhydrous tetrahydrofuran (50 mL). A solution of *t*-butylphenyltris(2-pyridyl)borate free acid (0.30 g, 0.79 mmol) and triethylamine (2.0 mL, 14 mmol) in methanol (10 mL) was then added. The reaction mixture was kept stirring for 3 h and subsequently filtered to give a red solution. The volatile components were removed on a rotary evaporator to give a red solid, which was purified by column chromatography on silica gel with hexanes as the eluent. Solvent evaporation gave the product as a red solid, which was dried under high vacuum at RT for 1 h. Yield: 0.22 g (60%). ^{1}H NMR (499.973 MHz, $CDCl_3$) δ = 8.09 (d, ^3J = 7.5 Hz, 4H, tPh-H2,6), 7.60 (d, ^3J = 8.0 Hz, 4H, tPh-H3,5), 7.59 (d, ^3J = 9.0 Hz, 6H, pyridyl-H3), 7.27 (pst, ^3J = 7.5 Hz, 6H, pyridyl-H4), 7.11 (d, ^3J = 5.5 Hz, 6H, pyridyl-H6), 6.44 (pst, ^3J = 6.5 Hz, 6H, pyridyl-H5), 1.52 (s, 18H, *t*-Bu). ^{13}C NMR (125.718 MHz, $CDCl_3$) δ = 188.0 (q, $^1J_{C-B}$ = 49.6 Hz, pyridyl-C2), 158.3 (pyridyl-C6), 149.2 (q, $^1J_{C-B}$ = 57.3 Hz, tPh–C1), 147.4 (tPh–C4), 136.7 (tPh–C2,6), 132.0 (pyridyl-C4), 125.7 (pyridyl-C3), 124.5 (tPh–C3,5), 119.7 (pyridyl-C5), 34.7 ($C(CH_3)_3$), 32.0 ($C(CH_3)_3$). ^{11}B NMR (160.411 MHz, $CDCl_3$) δ = −7.5 ($w_{1/2}$ = 21 Hz). UV–vis (25 °C, CH_2Cl_2): λ_{max} = 480 nm (ε = 16400 M^{-1} cm^{-1}), 425 (shoulder, ε = 11000 M^{-1} cm^{-1}). Cyclic voltammetry: $E_{1/2}$ = −350 mV, ΔE_p = 84 mV (1 mM, CH_2Cl_2 containing 0.1 M $[Bu_4N]PF_6$ as the supporting electrolyte; scan rate 100 mV/s). MALDI-TOF MS (benzo[α]pyrene): m/z = 812.356 (M^+, calcd for $^{12}C_{50}{}^1H_{50}{}^{11}B_2{}^{56}Fe^{14}N_6$ 812.363). Elemental analysis for crystals obtained from toluene: calcd for $C_{50}H_{50}B_2FeN_6{\cdot}C_7H_8$: C 75.68, H 6.46, N 9.29%; found C 75.61, H 6.46, N 9.24%. Single crystals of complex **2-Fe** for X-ray diffraction analysis were obtained by slow evaporation of a solution in toluene, CH_2Cl_2, or cyclohexane (heated to achieve dissolution).

Synthesis of Bis(*t*-butylphenyltris(2-pyridyl)borate) Manganese(II) (2-Mn). To a solution of *t*-butylphenyltris(2-pyridyl)-borate (0.30 g, 0.79 mmol) in methanol (10 mL) was added a solution of $MnCl_2$ (54 mg, 0.43 mmol) in methanol (5 mL). Triethylamine (1.0 mL) and hydrazine monohydrate (0.1 mL) were sequentially added into the reaction mixture. The resulting suspension was stirred for 5 min and then filtered. A yellow solid was collected, which was dried under high vacuum at RT and then extracted into toluene (120 mL). A small amount of insoluble components was removed by filtration and the product was obtained as a light yellow solid by solvent evaporation and drying under high vacuum. Yield: 0.20 g (62%). ^{1}H NMR (499.973 MHz, $CDCl_3$) δ = 35.0 (br, 6H, pyridyl-H), 17.6 (br, 6H, pyridyl-H), 9.6 (br, 4H, tPh), 7.5 (br, 4H, tPh), 1.34 (s, 18H, *t*-Bu), −6 (very br, 6H, pyridyl-H), −42.5 (br, 6H, pyridyl-H). ^{11}B NMR (160.411 MHz, $CDCl_3$) δ = −109.6 ($w_{1/2}$ = 150 Hz). High-resolution MALDI-MS (+ mode, benzo[α]pyrene): m/z = 811.3657 (M^+, 50%, calcd for $^{12}C_{50}{}^1H_{50}{}^{11}B_2{}^{55}Mn^{14}N_6$ 811.3658), 733.3318 (M^+-Py, 100%, calcd for $^{12}C_{45}{}^1H_{46}{}^{11}B_2{}^{55}Mn^{14}N_5$ 733.3314). Single crystals for X-ray diffraction analysis were obtained by slow evaporation of a saturated toluene solution.

Surface Area, Porosity, and Gas Uptake Measurement on 2-Mg. Following recrystallization of **2-Mg** from toluene, a portion of the crystals was subjected to solvent exchange in *n*-pentane to remove toluene from within the crystal lattice (following a procedure similar to that reported by Mastalerz[31]). The crystals were immersed in *n*-pentane for 24 h three times, and the solvent exchanged for fresh *n*-pentane each time. The sample was then evacuated for 20 h at 100 °C prior to performing gas sorption measurements.

■ ASSOCIATED CONTENT

Ⓢ Supporting Information

Additional experimental details. This material is available free of charge via the Internet at http://pubs.acs.org.

■ AUTHOR INFORMATION

Corresponding Author

*E-mail: fjaekle@rutgers.edu (F.J.), rogerlal@rutgers.edu (R.A.L.). Fax: +1 973 353 1264.

Notes

The authors declare no competing financial interest.

■ ACKNOWLEDGMENTS

This material is based upon work supported by the National Science Foundation under Grant CHE-0956655. The authors acknowledge partial support by NSF-CRIF Grant 0443538 for acquisition of the X-ray diffractometer used in these studies. We thank Prof. Jing Li, Haohan Wu, and Hao Wang at Rutgers University, New Brunswick campus, for acquisition of porosity and gas sorption data and Prof. John Sheridan for helpful discussions. F.J. thanks the Alfred P. Sloan foundation for a research fellowship.

■ REFERENCES

(1) (a) Trofimenko, S. *J. Am. Chem. Soc.* **1966**, *88*, 1842. (b) Trofimenko, S. *Chem. Rev.* **1993**, *93*, 943. (c) Trofimenko, S. *Scorpionates-The Coordination Chemistry of Polypyrazolylborate Ligands*; Imperial College Press: London, U.K., 1999; (d) Trofimenko, S. *Polyhedron* **2004**, *23*, 197.

(2) (a) Trofimenko, S. *J. Am. Chem. Soc.* **1967**, *89*, 6288. (b) Calabrese, J. C.; Trofimenko, S.; Thompson, J. S. *J. Chem. Soc., Chem. Commun.* **1986**, 1122.

(3) (a) White, D. L.; Faller, J. W. *J. Am. Chem. Soc.* **1982**, *104*, 1548. (b) Zagermann, J.; Kuchta, M. C.; Merz, K.; Metzler-Nolte, N. *Eur. J. Inorg. Chem.* **2009**, 5407.

(4) Reger, D. L.; Gardinier, J. R.; Gemmill, W. R.; Smith, M. D.; Shahin, A. M.; Long, G. J.; Rebbouh, L.; Grandjean, F. *J. Am. Chem. Soc.* **2005**, *127*, 2303.

(5) Recent examples: (a) Zhang, F.; Morawitz, T.; Bieller, S.; Bolte, M.; Lerner, H.-W.; Wagner, M. *Dalton Trans.* **2007**, 4594. (b) Camerano, J. A.; Casado, M. A.; Ciriano, M. A.; Oro, L. A. *Dalton Trans.* **2006**, 5287. (c) Hamon, P.; Thépot, J.-Y.; Le Floch, M.; Boulon, M.-E.; Cador, O.; Golhen, S.; Ouahab, L.; Fadel, L.; Saillard, J.-Y.; Hamon, J.-R. *Angew. Chem., Int. Ed.* **2008**, *47*, 8687. (d) Jové, F. A.; Pariya, C.; Scoblete, M.; Yap, G. P. A.; Theopold, K. H. *Chem.—Eur. J.* **2011**, *17*, 1310. (e) Scepaniak, J. J.; Vogel, C. S.; Khusniyarov, M. M.; Heinemann, F. W.; Meyer, K.; Smith, J. M. *Science* **2011**, *331*, 1049. (f) Qin, Y.; Cui, C.; Jäkle, F. *Macromolecules* **2008**, *41*, 2972.

(6) Cui, C.; Lalancette, R. A.; Jäkle, F. *Chem. Commun.* **2012**, *48*, 6930.

(7) For some excellent reviews of tris(2-pyridyl) tripod ligands with other bridge atoms (e.g., C, Si, Sn, Pb, N, P, As, Al, In), see: (a) Simmonds, H. R.; Wright, D. S. *Chem. Commun.* **2012**, *48*, 8617. (b) Szczepura, L. F.; Witham, L. M.; Takeuchi, K. J. *Coord. Chem. Rev.* **1998**, *174*, 5.

(8) (a) Pt complexes of bis(2-pyridylborate)s have been successfully applied in C-H activation. See, for example: Khaskin, E.; Zavalij, P. Y.; Vedernikov, A. N. *J. Am. Chem. Soc.* **2006**, *128*, 13054. (b) For the use of tripodal tri(2-oxazolinyl)borates in catalysis, see: Dunne, J. F.; Neal, S. R.; Engelkemier, J.; Ellern, A.; Sadow, A. D. *J. Am. Chem. Soc.* **2011**, *133*, 16782.

(9) (a) Fustin, C.-A.; Guillet, P.; Schubert, U. S.; Gohy, J.-F. *Adv. Mater.* **2007**, *19*, 1665. (b) Abd-El-Aziz, A. S., Manners, I., Eds.; *Frontiers in Transition Metal-Containing Polymers*; Wiley-Interscience: Hoboken, NJ, 2007; (c) Burnworth, M.; Knapton, D.; Rowan, S. J.; Weder, C. *J. Inorg. Organomet. Polym. Mater.* **2007**, *17*, 91. (d) Manners, I. *Angew. Chem., Int. Ed.* **2007**, *46*, 1565.

(10) For related studies with Tp ligand-functionalized polymers, see: Qin, Y.; Shipman, P. O.; Jäkle, F. *Macromol. Rapid Commun.* **2012**, *33*, 562−567.

(11) (a) Lee, J.; Farha, O. K.; Roberts, J.; Scheidt, K. A.; Nguyen, S. T.; Hupp, J. T. *Chem. Soc. Rev.* **2009**, *38*, 1450. (b) Li, J.-R.; Kuppler, R. J.; Zhou, H.-C. *Chem. Soc. Rev.* **2009**, *38*, 1477. (c) Murray, L. J.; Dincă, M.; Long, J. R. *Chem. Soc. Rev.* **2009**, *38*, 1294.

(12) Hertzsch, T.; Hulliger, J.; Weber, E.; Sozzani, P. Organic Zeolites. In *Encyclopedia of Supramolecular Chemistry*; Atwood, J. L., Steed, J. W., Eds.; Marcel Dekker: New York, 2004; pp 996−1005.

(13) Barbour, L. J. *Chem. Commun.* **2006**, 1163.

(14) (a) Tian, J.; Thallapally, P. K.; McGrail, B. P. *CrystEngComm* **2012**, *14*, 1909. (b) Mastalerz, M. *Chem.—Eur. J.* **2012**, *18*, 10082 , and references cited therein.

(15) Mastalerz, M. *Angew. Chem., Int. Ed.* **2012**, *51*, 584.

(16) Sozzani, P.; Bracco, S.; Comotti, A.; Ferretti, L.; Simonutti, R. *Angew. Chem., Int. Ed.* **2005**, *44*, 1816.

(17) Alvarez, C. S.; Garcia, F.; Humphrey, S. M.; Hopkins, A. D.; Kowenicki, R. A.; McPartlin, M.; Layfield, R. A.; Raja, R.; Rogers, M. C.; Woods, A. D.; Wright, D. S. *Chem. Commun.* **2005**, 198.

(18) (a) Eichhorn, D. M.; Armstrong, W. H. *Inorg. Chem.* **1990**, *29*, 3607. (b) Halcrow, M. A.; Brechin, E. K.; McInnes, E. J. L.; Mabbs, F. E.; Davies, J. E. *J. Chem. Soc., Dalton Trans.* **1998**, 2477. (c) Kitano, T.; Sohrin, Y.; Hata, Y.; Kawakami, H.; Hori, T.; Ueda, K. *J. Chem. Soc., Dalton Trans.* **2001**, 3564. (d) Jeitler, J. R.; Turnbull, M. M.; Wikaira, J. L. *Inorg. Chim. Acta* **2003**, *351*, 331. (e) Zhao, N.; van Stipdonk, M. J.; Bauer, C.; Campana, C.; Eichhorn, D. M. *Inorg. Chem.* **2007**, *46*, 8662. (f) Duboc, C.; Collomb, M.-N.; Pécaut, J.; Deronzier, A.; Neese, F. *Chem.—Eur. J.* **2008**, *14*, 6498. (g) Misra, P.; Liao, C.-Y.; Wei, H.-H.; Mohanta, S. *Polyhedron* **2008**, *27*, 1185. (h) Sjödin, M.; Gätjens, J.; Tabares, L. C.; Thuéry, P.; Pecoraro, V. L.; Un, S. *Inorg. Chem.* **2008**, *47*, 2897.

(19) Kucharski, E. S.; McWhinnie, W. R.; White, A. H. *Aust. J. Chem.* **1978**, *31*, 53.

(20) Anderson, P. A.; Astley, T.; Hitchman, M. A.; Keene, F. R.; Moubaraki, B.; Murray, K. S.; Skelton, B. W.; Tiekink, E. R. T.; Toftlund, H.; White, A. H. *Dalton Trans.* **2000**, 3505.

(21) Although $[Fe\{Al(2\text{-}py)_3\}_2]$ was reported to crystallize in the $R\bar{3}$ space group and contains solvent-filled channels, the latter are rectangular rather than hexagonal and even smaller in size (shortest H···H distances of 3.37, 5.02 Å) than those found for the toluene solvate of **Fe-2**. See ref 17.

(22) Related structures based on a $[M(terpy)_2]^{2+}$ derivatives have been reported: Beves, J. E.; Constable, E. C.; Housecroft, C. E.; Neuburger, M.; Schaffner, S.; Zampese, J. A. *Polyhedron* **2009**, *28*, 3828 In those cases, the complexes are positively charged, resulting in the incorporation of not only solvent molecules but also counteranions that are difficult if not impossible to remove.

(23) Spek, A. L. *J. Appl. Crystallogr.* **2003**, *36*, 7.

(24) Nishio, M.; Hirota, M.; Umezawa, Y. *The CH/π Interaction. Evidence, Nature and Consequences*; Wiley-VCH: New York, 1998.

(25) Cooper, A. I. *Angew. Chem., Int. Ed.* **2012**, *51*, 7892.

(26) (a) Allcock, H. R.; Siegel, L. A. *J. Am. Chem. Soc.* **1964**, *86*, 5140. (b) Sozzani, P.; Comotti, A.; Simonutti, R.; Meersmann, T.; Logan, J. W.; Pines, A. *Angew. Chem., Int. Ed.* **2000**, *39*, 2695.

(27) Comotti, A.; Bracco, S.; Distefano, G.; Sozzani, P. *Chem. Commun.* **2009**, 284.

(28) Lim, S.; Kim, H.; Selvapalam, N.; Kim, K.-J.; Cho, S. J.; Seo, G.; Kim, K. *Angew. Chem., Int. Ed.* **2008**, *47*, 3352.

(29) Bezzu, C. G.; Helliwell, M.; Warren, J. E.; Allan, D. R.; McKeown, N. B. *Science* **2010**, *327*, 1627.

(30) (a) Yang, W.; Greenaway, A.; Lin, X.; Matsuda, R.; Blake, A. J.; Wilson, C.; Lewis, W.; Hubberstey, P.; Kitagawa, S.; Champness, N. R.; Schröder, M. *J. Am. Chem. Soc.* **2010**, *132*, 14457. (b) Crane, A. K.; MacLachlan, M. J. *Eur. J. Inorg. Chem.* **2012**, *2012*, 17. (c) Raatikainen, K.; Rissanen, K. *Chem. Sci.* **2012**, *3*, 1235.

(31) Mastalerz, M.; Oppel, I. M. *Angew. Chem., Int. Ed.* **2012**, *51*, 5252.

(32) (a) Huang, Z.; White, P. S.; Brookhart, M. *Nature* **2010**, *465*, 598. (b) He, Y.; Xiang, S.; Chen, B. *J. Am. Chem. Soc.* **2011**, *133*, 14570. (c) Lusi, M.; Barbour, L. J. *Angew. Chem., Int. Ed.* **2012**, *51*, 3928.

(33) Msayib, K. J.; Book, D.; Budd, P. M.; Chaukura, N.; Harris, K. D. M.; Helliwell, M.; Tedds, S.; Walton, A.; Warren, J. E.; Xu, M.; McKeown, N. B. *Angew. Chem., Int. Ed.* **2009**, *48*, 3273.

(34) Qin, Y.; Kiburu, I.; Shah, S.; Jäkle, F. *Org. Lett.* **2006**, *8*, 5227.

(35) Sheldrick, G. *SHELXTL* (5.10); Bruker XRD: Madison, WI.

(36) Sheldrick, G. M. *SADABS, Multi-Scan Absorption Correction Program*, Version 2.; University of Göttingen: Göttingen, Germany, 2008.